Constraint on the primordial vector mode and its magnetic field generation from seven-year Wilkinson Microwave Anisotropy Probe Observations

Kiyotomo Ichiki,[1, *] Keitaro Takahashi,[2] and Naoshi Sugiyama[1, 3, 4]

[1]*Department of Physics and Astrophysics, Nagoya University, Nagoya 464-8602, Japan*
[2]*Department of Physics, Kumamoto University, Kumamoto 860-8555, Japan*
[3]*Kobayashi-Maskawa Institute for the Origin of Particles and the Universe,*
Nagoya University, Chikusa-ku, Nagoya, 464-8602, Japan
[4]*Institute for the Physics and Mathematics of the Universe (IPMU),*
The University of Tokyo, Chiba 277-8582, Japan
(Dated: December 21, 2011)

A primordial vector mode and its associated magnetic field generation are investigated. Firstly, we put an observational constraint on the amount of the primordial vector mode from the seven-year WMAP data. The constraint is found as $r_v \lesssim -\frac{r}{40} + 0.012$, where r_v and r are the amounts of vector and tensor perturbation amplitudes with respect to the scalar one, respectively. Secondly, we calculate the spectrum of magnetic fields inevitably created from the primordial vector mode, given the constraint on r_v. It is found that the maximum amount of magnetic fields generated from the vector mode is given by $B \lesssim 10^{-22}\mathrm{G} \left(\frac{r_v}{0.012}\right)^{1/2} \left(\frac{k}{0.002}\right)^{(n_v+1)/2}$ with n_v being a spectral index of the vector mode. We find a non-trivial cancellation of the magnetic field generation in the radiation dominated era, which creates a characteristic cut off in the magnetic field spectrum around $k \approx 1.0$ Mpc^{-1}.

PACS numbers: 98.70.Vc, 95.30.-k, 98.80.Es

I. INTRODUCTION

There are observational evidences which indicate that magnetic fields exist not only in galaxies, but also in even larger systems, such as cluster of galaxies and intra-cluster spaces [1]. Yet, the origin of such large scale magnetic fields is still a mystery [1]. It is now widely believed that the magnetic fields at large scales are amplified from a tiny field and maintained by the hydro-magnetic processes, i.e., the dynamo. However, the dynamo needs a seed field to act on and does not explain the origin of magnetic fields itself. As far as the magnetic fields in galaxies are concerned, the seed fields as large as $10^{-20} \sim 10^{-30}$ G are required in order to account for the observed fields [2] of order 1μ G at the present universe. Recent discovery of magnetic fields in galaxies at high redshifts [3] may require even larger seed fields.

A classical way to generate seed magnetic fields in astrophysics is based on the Biermann battery effect [4]. The Biermann battery works in various astrophysical systems, such as stars [5], supernova remnants [6, 7], protogalaxies [8], large-scale structure formation [9], and ionization fronts at cosmological recombination [10, 11]. These studies show that magnetic fields with amplitude $10^{-16} \sim 10^{-21}$ G could be generated. However, the coherence-length of seed fields generated by such astrophysical mechanisms may tend to be too small to account for galaxy-scale magnetic fields.

On the other hand, cosmological mechanisms at the early inflationary epoch can produce magnetic fields with a large coherence length since accelerating expansion during inflation can stretch small-scale fields to scales that can exceed the causal horizon [12–15]. However, because no magnetic field is generated in simplest models with the usual electromagnetic field, it is necessary to introduce some extensions to the standard particle model. Furthermore, it is recently argued that the backreactions from the electro-magnetic fields will stop the inflation and significantly suppress the magnetic field generation [16, 17], if they are properly taken into account.

Generation mechanisms of magnetic fields in a decelerating universe prior to cosmological recombination have also been proposed. Originally, Harrison found that the vorticity in a primordial plasma can generate magnetic fields [18]. This is because electrons and ions would tend to spin at different rates as the universe expands due to the radiation drag on electrons, arising a rotation-type electric current and thus inducing magnetic fields. Following his idea, many authors have investigated magnetic field generation through the second order vorticity generated from the first order density perturbations [19–27].

In this paper, we consider a first order vector (vorticity) mode firstly investigated by Rebhan followed by Lewis [28, 29]. In a Friedmann universe with a perfect fluid without anisotropic stress, the vector mode has only a decaying mode. This means a diverging vector metric perturbation (frame-dragging potential) at the initial time and therefore the model is inconsistent with an almost isotropic Friedmann universe, and goes beyond the linear perturbation theory. However, in the existence of anisotropic stress by free streaming particles such as neutrinos, it has been found that there exists a regular (growing) mode with an initial non-zero vorticity and with isotropic initial phase space distributions. We first present an observational constraint on this primordial vector mode amplitude using the seven-year WMAP data. We then estimate the amplitude of the magnetic fields inevitably created from this vector mode in the light of the obtained constraint on the vector mode amplitude.

This paper is organized as follows. In Sec. II, the overview of the primordial vector mode investigated by [28, 29] is described and we give an analytic solution obtained by a tight coupling approximation. In Sec. III, we show the constraints on the vector mode amplitude and its spectral index from the seven-year WMAP data and discuss its implication. In Sec. IV, we calculate the magnetic field spectrum inevitably generated from the primordial vector mode. Finally, Sec. V is devoted to the summary and discussion.

II. EQUATIONS AND SOLUTIONS

A. preliminary

Here we quickly review basic equations for the evolution of primordial vector modes. We consider linear perturbations in the synchronous gauge, in a flat Friedmann-Robertson-Walker universe with a metric

$$ds^2 = a(\eta)^2 \left[-d\eta^2 + (\delta_{ij} + h_{ij})dx^i dx^j \right] , \tag{1}$$

where $a(\eta)$ is a scale factor. Because we are interested in the vector mode, the metric perturbations h_{ij} are decomposed in Fourier space as

$$h_{ij} = i\hat{k}_i h_j^V + i\hat{k}_j h_i^V , \tag{2}$$

where h_i^V is divergence-less, i.e., $\hat{k}^i h_i^V = 0$. It is useful to expand the vector h_i^V in terms of two independent transverse basis vectors as

$$h_i^V(\vec{k}) = \sum_{\pm} h_{\pm}^V(\vec{k}) e_i^{\pm}(\vec{k}) , \tag{3}$$

where $\pm$ represents the parity. Because each parity component and each Fourier mode evolve independently, we omit $\vec{k}$ and $\pm$ dependencies for simplicity in the rest of the paper. Let us work with the gauge invariant metric variable, σ, which is defined using the synchronous gauge variable h^V as $\sigma \equiv \dot{h}^V/k$. Then, the linearized Einstein equations give

$$k^2\sigma = -16\pi G a^2 \left(\bar{\rho} + \bar{P} \right) v , \tag{4}$$

$$\dot{\sigma} + 2\mathcal{H}\sigma = 8\pi G a^2 \bar{P}\pi/k , \tag{5}$$

where dot denotes a derivative with respect to the conformal time η, $\mathcal{H} = \dot{a}/a$ is the conformal Hubble parameter, $\bar{\rho}$ and $\bar{P}$ are the zero-th order density and pressure of the total fluid, respectively, and v and π are the velocity and anisotropic stress in the vector mode, respectively. From Eq.(5) it is readily found that the vector metric perturbation has only a decaying mode $\sigma \propto a^{-2}$ if there is no anisotropic stress.

For the matter part, the Euler equation of baryon is given by

$$\dot{v}_b + \mathcal{H}v_b = -\frac{4\rho_\gamma}{3\rho_b} a n_e \sigma_T \left(v_b - v_\gamma \right) , \tag{6}$$

where n_e is the electron number density and σ_T is the Thomson scattering cross section. For the photons we expand the distribution function for the vector mode into multipoles and rewrite the Boltzmann equation as

$$\dot{v}_\gamma + \frac{1}{8}k\pi_\gamma = -a n_e \sigma_T \left(v_\gamma - v_b \right) , \tag{7}$$

$$\dot{\pi}_\gamma + \frac{8}{5}kI_3 - \frac{8}{5}kv_\gamma = -a n_e \sigma_T \left(\frac{9}{10}\pi_\gamma - \frac{9}{5}E_2 \right) - \frac{8}{5}k\sigma , \tag{8}$$

$$\dot{I}_\ell + k\frac{\ell}{2\ell+1} \left(\frac{\ell+2}{\ell+1}I_{\ell+1} - I_{\ell-1} \right) = -a n_e \sigma_T I_\ell \ \ (\ell > 2) , \tag{9}$$

where I_ℓ is the ℓ-th order angular moment of the photon distribution, and E_ℓ is the ℓ-th order moment of the E-mode polarization [29].

B.   tight coupling approximation and solutions

In the very early universe photons and baryons are tightly coupled as the opacity $\frac{1}{\dot{\tau}} = a n_e \sigma_T$ is large. This enables us to expand the equations by a tight coupling parameter,

$$\epsilon = \frac{k}{\dot{\tau}} \sim 10^{-2} \left(\frac{k}{1\text{Mpc}} \right) \left(\frac{1+z}{10^4} \right)^{-2} \left(\frac{\Omega_b h^2}{0.02} \right)^{-1} , \tag{10}$$

where Ω_b is the baryon density normalized by the critical density, and h is the Hubble parameter normalized by 100 km/s/Mpc. At the lowest order, the equation for photon velocity is

$$\dot{v}_\gamma^{(0)} = -\frac{\dot{R}}{1+R} v_\gamma^{(0)} , \tag{11}$$

where $R = \frac{3\rho_b}{4\rho_\gamma}$. The solution is

$$v_\gamma^{(0)} = \frac{v_{\gamma,\text{ini}}}{1+R} , \tag{12}$$

where $v_{\gamma,\text{ini}}$ is the initial photon velocity. Therefore, the fluid velocity stays constant deep in the radiation dominated era where $R \ll 1$. At this order the baryon-photon slip and the photon anisotropic stress do not exist. At next order they are given by

$$v_\gamma^{(1)} - v_b^{(1)} = \frac{k}{\dot{\tau}} \frac{R\mathcal{H}}{k(1+R)} v_\gamma^{(0)} , \tag{13}$$

$$\pi_\gamma^{(1)} = \frac{k}{\dot{\tau}} \frac{32}{15} \left(v_\gamma^{(0)} + \sigma^{(0)} \right) , \tag{14}$$

respectively, where $\sigma^{(0)}$ is the solution of the vector metric perturbation at the lowest order. Note that the transfer of baryon-photon slip is independent of k. In other words, because $\dot{R} \approx R/\tau$ the slip term in the vector mode is further suppressed by a factor of $R/(k\tau)$ on small scales. This is compared with the slip term in the scalar mode, i.e. $v_\gamma - v_b \propto (k/\dot{\tau})R$, where the k dependence derives from the pressure gradient.

For the later discussion about magnetic field generation we derive the baryon-photon slip at the next order in the tight coupling approximation. We find it to be

$$
\begin{aligned}
v_\gamma^{(2)} - v_b^{(2)} = {} & \frac{k}{\dot{\tau}} \frac{R\mathcal{H}}{(1+R)k} v_\gamma^{(1)} - \frac{4}{15} \left(\frac{k}{\dot{\tau}} \right)^2 \frac{R}{1+R} \left(v_\gamma^{(0)} + \sigma^{(0)} \right) \\
& + \frac{R^2}{(1+R)^2} \frac{\mathcal{H}}{\dot{\tau}} \frac{k}{\dot{\tau}} \frac{v_\gamma^{(0)}}{k} \left[\frac{\dot{R}}{R(1+R)} + \frac{\dot{\mathcal{H}}}{\mathcal{H}} + \frac{\dot{v}_\gamma^{(0)}}{v_\gamma^{(0)}} - \frac{\ddot{\tau}}{\dot{\tau}} + \mathcal{H} \right] .
\end{aligned}
\tag{15}
$$

Therefore, up to the second order in the tight coupling approximation the baryon-photon slip is given by

$$v_\gamma - v_b = \frac{k}{\dot{\tau}} \frac{R\mathcal{H}}{(1+R)k} v_\gamma - \frac{4}{15} \left(\frac{k}{\dot{\tau}} \right)^2 \frac{R}{1+R} (v_\gamma + \sigma) , \tag{16}$$

where we have neglected cosmological redshift terms. Note that the signs of the two terms are different. We shall see below that, because of this, a significant amount of magnetic fields resolves away when the two terms become comparable around the Silk damping epoch.

Before moving to the next section we summarize the initial conditions [28, 29]. By expanding the equations in powers of $k\tau$ and assuming the radiation dominated era, we find at the lowest order

$$\sigma_{\text{ini}} = \sigma_0 , \tag{17}$$

$$v_{\gamma,\text{ini}} = \sigma_0 \left(\frac{4R_\nu + 5}{4R_\gamma} \right) , \tag{18}$$

$$v_{\nu,\text{ini}} = -\frac{R_\gamma}{R_\nu} v_{\gamma,\text{ini}} , \tag{19}$$

$$v_{b,\text{ini}} = v_{\gamma,\text{ini}} , \tag{20}$$

$$\pi_{\nu,\text{ini}} = -\frac{2}{R_\nu} \sigma_0 k\tau , \tag{21}$$

where we have defined the ratios $R_\nu = \frac{\rho_\nu}{\rho_\nu + \rho_\gamma}$ and $R_\gamma = 1 - R_\nu$. Evolutions of the vector perturbations are presented in Fig. 1.
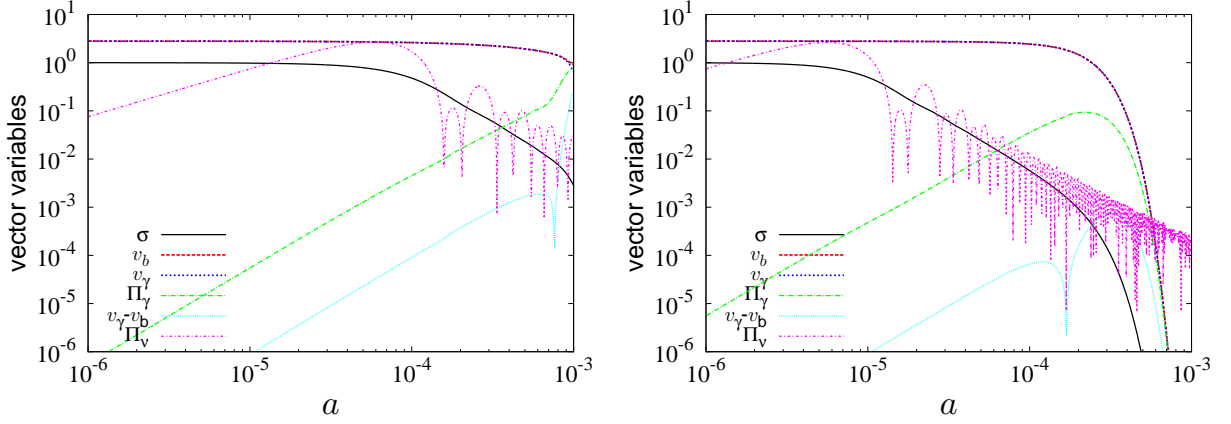
FIG. 1: Time evolutions of the vector perturbation variables with wavenumber $k = 0.1$ Mpc^{-1} (left) and $k = 1.0$ Mpc^{-1} (right). The vector potential σ starts to decay after horizon crossing, while velocities $v_{b,\gamma}$ stay constant until the Silk damping takes place.

III.   CMB CONSTRAINT ON THE PRIMORDIAL VECTOR MODE

In order to compare with the CMB data precisely, we use the CosmoMC package with a modification to include two new parameters, r_v and n_v. Here r_v is the vector-scalar ratio and n_v is the spectral index of the vector power spectrum. Specifically, we parameterize the power spectrum of primordial vector mode with an initial amplitude of the metric perturbation σ as

$$\frac{k^3}{2\pi^2} \left\langle \sigma(\vec{k})\sigma^*(\vec{k}') \right\rangle = \mathcal{P}_\sigma(k)\delta(\vec{k} - \vec{k}') = A_\sigma \left(\frac{k}{k_0} \right)^{n_v - 1} \delta(\vec{k} - \vec{k}') \, , \tag{22}$$

where $k_0 = 0.002$ Mpc^{-1} is the pivot scale. The vector-scalar ratio is defined by

$$r_v = \frac{A_\sigma}{A_s} \, , \tag{23}$$

where A_s is the scalar counterpart of the power spectrum amplitude.

The likelihood function we calculate is given by the WMAP collaboration [30, 31] and the codes are publicly available at their web site. To include the primordial vector mode, we calculate the angular power spectrum, $C_{\text{vector } \ell}$, of the CMB anisotropy of temperature and E-mode polarization auto-correlations (TT and EE) and their cross correlation (TE) using the CAMB code [32]. We add these power spectra to those from the scalar and tensor modes as

$$C_{\text{tot } \ell}^{\text{TT,TE,EE}} = C_{\text{scalar } \ell}^{\text{TT,TE,EE}} + C_{\text{tensor } \ell}^{\text{TT,TE,EE}} + C_{\text{vector } \ell}^{\text{TT,TE,EE}} \, , \tag{24}$$

where we have assumed that the primordial scalar, vector and tensor modes are statistically independent. Then $C_{\text{tot } \ell}$ are fitted to the CMB data. The B-mode polarization angular power spectrum is not used for our analysis because the sensitivity of the current observational data of B-mode polarization is not enough to give limits on the vector or tensor mode amplitudes.

In Fig 2, we depict the CMB angular power spectra along with the seven-year WMAP data. In that figure, the parameters of the primordial vector mode are fixed to $r_v = 9.45 \times 10^{-3}$ and $n_v = 0.921$, respectively, which are the allowed values at 95% confidence levels (red dashed lines in Fig.2). The spectra look similar to those from the tensor mode perturbations, although the powers extend to the higher multipoles without oscillatory features. As clearly seen from the figure, the current constraints are mainly placed on from the TT power spectrum at low multipoles if the vector mode is nearly scale invariant. The situation is the same with the case of the current constraint on the primordial tensor mode (gravitational waves) from the CMB power spectrum. Only in the panel for the TT power spectrum we also show the case with a bluer spectral index $n_v = 2.0$ with $r_v = 1.0 \times 10^{-3}$, which are also at the edge of 95% confidence levels. In this case, we find that the constraint again comes from TT power spectrum, but at the higher multipoles around $\ell \approx 1000$.

The correlation between the parameters of primordial vector modes, r_v and n_v, is shown in the right panel of Fig 3. If the primordial vector perturbation is given almost scale invariant, we found that the constraint is put at lowest
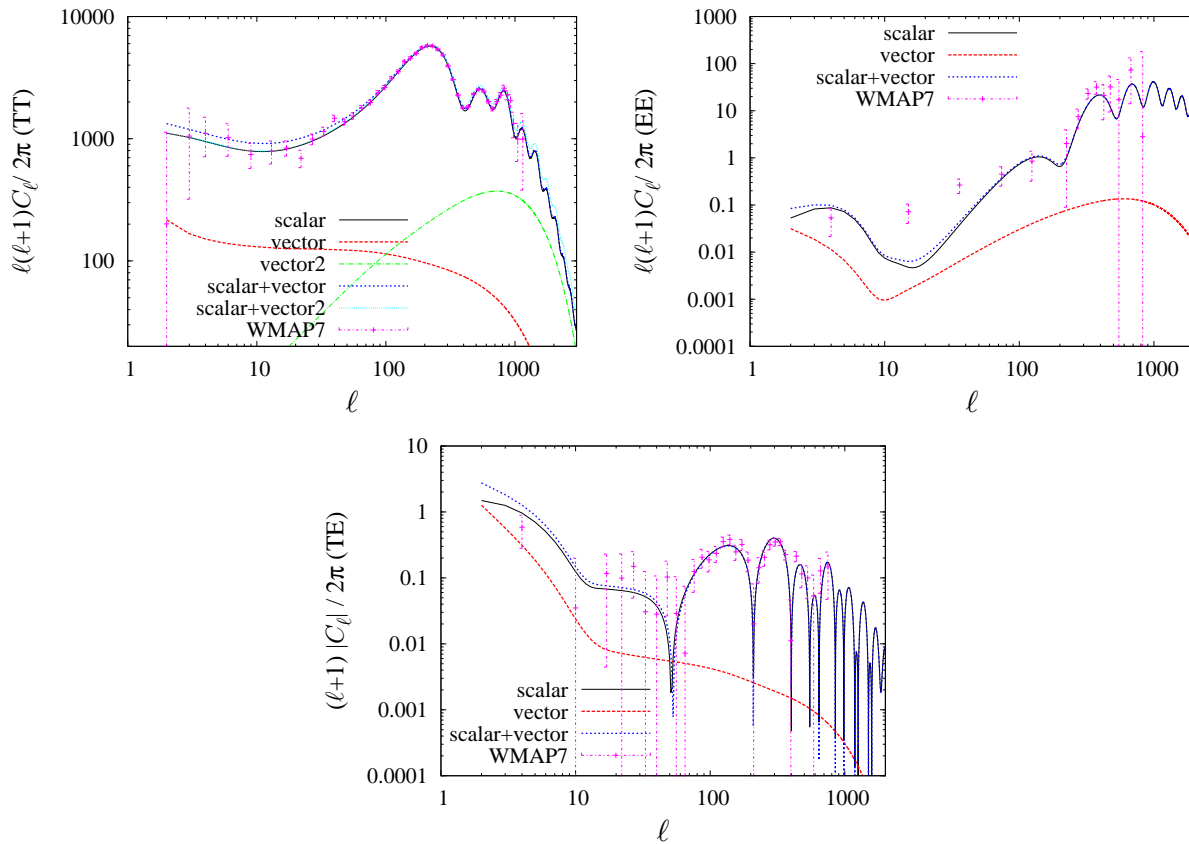
FIG. 2: CMB angular anisotropies power spectra, temperature (TT), E-mode polarization (EE), and their cross-correlation (TE), induced by scalar and vector type perturbations. The constraint mainly comes from the TT angular power spectrum. The vector mode parameters are taken as $(r_v, n_v) = (0.945 \times 10^{-2}, 0.921)$ and $(1.0 \times 10^{-3}, 2.0)$ for red dashed lines and green dash-dotted line (TT spectrum only), respectively.

multipoles as mentioned above and the constraint is the weakest. When the spectrum becomes bluer as $n_v \gtrsim 1$, the constraint comes from the higher multipoles and hence it becomes tighter. For example, when $n_v \approx 2.0$ the constraint becomes $r_v \lesssim 0.001$, while $r_v \lesssim 0.009$ when $n_v \approx 1.0$.

To make our analysis as general as possible, we made our Markov chain analysis with and without the primordial tensor mode. The effect of including the tensor mode on the constraint on the vector mode is also shown in the right panel of Fig. 3. We observe that the constraint on the vector mode generally becomes tighter if the tensor mode is included. The constraints we found are $r_v \lesssim 9.45 \times 10^{-3}$ (without tensor) and $r_v \lesssim 8.36 \times 10^{-3}$ (with tensor) when the all the other parameters are marginalized. The simultaneous constraint on the vector and tensor modes is shown in the left panel of Fig. 3. The result shown is easily understood: because the angular power spectra of temperature anisotropies from the vector and tensor modes are similar, the current CMB data can put constraint on the total amount of the vector and tensor mode perturbations. We found the constraint to be

$$r_v + \left(\frac{r}{40}\right) \lesssim 0.012 \,, \tag{25}$$

at 95.4% confidence level where r stands for the tensor-scalar ratio.

IV. MAGNETIC FIELD GENERATION

When there exists velocity difference between baryons and photons in the vector mode, magnetic fields may be generated inevitably. This arises because photons scatter off electrons preferable to protons. Electric fields are induced to prevent charge separation between electrons and protons, and magnetic fields are generated from these induced electric fields through Maxwell equations if there exists the vorticity difference. In general, magnetic fields then affect the evolution of the fluids. However, we omit any backreactions from magnetic fields on the fluid motion
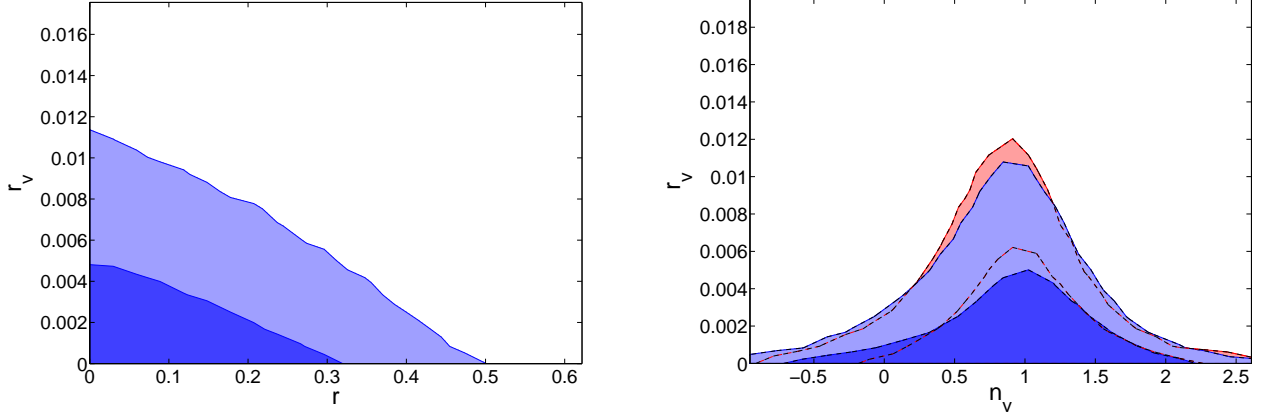
FIG. 3: 68 % and 95 % confidence regions from WMAP 7-yr data on r-r_v (left) and n_v-r_v planes (right). Left panel shows that constraint is on the total amount of vector and scalar components. Right panel shows constraints become severer when vector perturbation spectrum gets away from scale invariant $n_v = 1$. In that panel red contours are obtained from the analysis without tensor modes, blue contours are obtained including tensors. Blue and red spectra are allowed when $r_v \to 0$.

because we are interested in the magnetic field generation from zero and thus the backreactions from the magnetic fields will be negligible. In terms of the cosmological perturbation theory, the backreactions from magnetic fields are second order, namely, the Lorentz force would be $vB \sim \mathcal{O}(v^2)$ and the energy momentum tensor will be proportional to $B^2 \sim \mathcal{O}(v^2)$.

The evolution equation of magnetic fields due to the Thomson scattering is given by

$$\frac{d(a^2 B^i)}{dt} = \frac{4\sigma_T \rho_\gamma a}{3e} \epsilon^{ijk} \left(v_{\gamma\ j,k} - v_{b\ j,k} \right) , \tag{26}$$

where ϵ^{ijk} is the Levi-Civita tensor and e is the electric charge. For the scalar type perturbation, this term vanishes because $\epsilon^{ijk} v_{j,k}^S \sim \epsilon^{ijk} \hat{k}_j \hat{k}_k v^S = 0$. In this paper we solve the above equation with the initial condition $B = 0$ at $z = 10^9$, which roughly corresponds the time of neutrino decoupling.

Even in the case where the vector mode perturbation exists, the mean of the magnetic fields should still be zero, but there exists the variance. To find the spectrum of magnetic fields, we first calculate $B^i B_i$. That is given by

$$a^4 B^i(\vec{k}, t) B_i^*(\vec{k'}, t) = \left(\frac{4\sigma_T}{3e} \right)^2 \left(\delta^{j\ell} \delta^{km} - \delta^{jm} \delta^{k\ell} \right) k_k k_m' \int \int a(t') \delta v_j(\vec{k}, t') a(t'') \delta v_\ell^*(\vec{k}, t'') dt' dt'' . \tag{27}$$

Taking the ensemble average of this expression and defining the vector power spectrum as

$$\left\langle \delta v_j(\vec{k}, t') \delta v_\ell^*(\vec{k'}, t'') \right\rangle = \frac{2\pi^2}{k^3} \mathcal{P}_\sigma(k) P_{j\ell}(\hat{k}) \delta v(k, t') \delta v(k, t'') \delta(\vec{k} - \vec{k'}) \tag{28}$$

$$P_{j\ell}(\hat{k}) = \delta_{j\ell} - \hat{k}_j \hat{k}_\ell , \tag{29}$$

where $\delta v(k, t)$ is the transfer function of baryon-photon slip with $\sigma = 1$ at the initial time, and the magnetic field power spectrum can be written as

$$a^4(t) \frac{k^3}{2\pi^2} S_B(k, t) = \left(\frac{4\sigma_T}{3e} \right)^2 2\mathcal{P}_\sigma(k) k^2 \left[\int dt' a(t') \rho_\gamma(t') \delta v(k, t') \right]^2 . \tag{30}$$

Here, magnetic field power spectrum $S_B(k)$ is defined as

$$S_B(k) \delta(\vec{k} - \vec{k'}) = \left\langle B^i(\vec{k}) B_i(\vec{k'}) \right\rangle . \tag{31}$$

We numerically calculate the magnetic field spectra and show them in Fig. 4. In that figure, we took the vector mode parameters as $r_v = 0.01$ and $n_v = 1$, which give the maximum amount of the vector mode allowed at large scales.

First of all, let us roughly estimate the amplitude of the generated magnetic fields. From Eq.(26), it is estimated as

$$
\begin{aligned}
(a^2 B) &\simeq \left(\frac{4\sigma_T}{3e}\right)\frac{a}{H}\rho_\gamma k(v_\gamma - v_b)\ , \\
&\simeq \left(\frac{4\sigma_T}{3e}\right)a^2\rho_\gamma\left(\frac{k}{\dot{\tau}}\right)\frac{R}{(1+R)^2}\left(\frac{4R_\nu+5}{4R_\gamma}\right)\sigma_0, \\
&\sim \left(\frac{4\sigma_T}{3e}\right)a^2\rho_\gamma\left(\frac{k}{\dot{\tau}}\right)\sigma_0
\end{aligned}
\tag{32}
$$

where H is the usual Hubble parameter and we have used the tight coupling solution for $(v_\gamma - v_b)$ derived in Sec. II. By substituting Eq.(10), $\rho_\gamma \simeq 2 \times 10^{-51}(1+z)^4$ [GeV^4], and $\sigma_T \simeq 1.7 \times 10^3$ [GeV^{-2}], we find

$$
a^2 B \sim 1.2 \times 10^{-27}\mathrm{G}\left(\frac{k}{\mathrm{Mpc}^{-1}}\right)\left(\frac{1+z}{10^4}\right)^{-1}\left(\frac{r_v}{0.01}\right)^{1/2}\ .
\tag{33}
$$

Therefore, around the cosmological recombination epoch, $B \sim 10^{-21}$ G is expected for the magnetic field strength.

At super-horizon scales, the magnetic fields have a power-law $B \propto k$ if the vector mode power spectrum is scale invariant. This is manifestly shown by Eq.(32). If the primordial vector mode is tilted as $n_v \neq 1$, the magnetic field spectrum at super horizon scale should become as $B \propto k^{(n_v+1)/2}$.

At subhorizon scales, we found some interesting features in the resultant magnetic field spectrum. First, in the radiation dominated era, there is a peak just above the Silk damping scale. Secondly, we find a characteristic cut-off below the Silk damping scale. These features were not observed in the magnetic field spectrum from the second order vector modes. In that case the magnetic field spectrum is extended toward much smaller scales [24–26]. In the primordial vector mode considered here there is no significant difference in the evolution of velocity difference between photons and baryons before and after the horizon crossing. Therefore the magnetic fields continue to grow after the horizon crossing, which is manifestly shown in the magnetic field spectrum as $B \propto k$ for $k \gtrsim k_h$, with k_h being the wavenumber corresponding to the Hubble scale. It is expected that the generation of magnetic fields ceases around the Silk damping epoch where the velocity difference, $v_\gamma - v_b$, reaches its maximum value and starts to diminish. The peak position and the amplitude of magnetic fields there can be estimated as follows. The magnetic fields generated from Eq.(26) is estimated as

$$
\mathcal{B} \equiv (a^2 B) \approx \frac{a}{H}\rho_\gamma k(v_\gamma - v_b) \propto ka\ ,
\tag{34}
$$

where we have defined the comoving magnetic field $\mathcal{B}$, and used the relations in the radiation dominated era such as $H \propto a^{-2}$, $\rho_\gamma \propto a^{-4}$, and $(v_\gamma - v_b) \propto a^2$. The comoving magnetic fields evolve in time as $\propto a$ and therefore the maximum value is reached at the Silk scale where the perturbations start to be erased. Because the diffusion scale is scaled as $k_{\mathrm{diff}} \propto a^{-3/2}$ [33], the scale factor when diffusion damping occurs at a given scale k is given as $a_{\mathrm{Silk}} \propto k^{-2/3}$. Therefore, if the magnetic field generation just ceased when the Silk damping started we should expect that the magnetic fields have the spectrum as $\mathcal{B} \propto ka_{\mathrm{Silk}} \propto k^{1/3}$. In Fig. 4 we find that the peak amplitudes at different redshifts are indeed on this scaling relation.

However, we found a non-trivial cancellation of the magnetic field generation. In fact, the magnetic field generation does not only cease at the Silk damping epoch, but a significant amount of magnetic fields generated by that time vanishes as is shown in the right panel of Fig. 5. This happens because the sign of the velocity difference, $v_\gamma - v_b$, flips at the onset of the Silk damping, which is shown in the left panel of Fig. 5. Deep in the radiation dominated era, the velocity of radiation (photon) fluid stays constant due to the redshift of energy density (Eq. (12)), while the velocity of baryon fluid should decay as $v_b \propto a^{-1}$ if baryons had no interaction with photons. Therefore during that time the baryon fluid is dragged by the photon fluid, and we expect that $v_\gamma - v_b > 0$ if $v_{\gamma,\mathrm{ini}} > 0$. After the diffusion damping starts to erase the perturbations in photons, the baryon fluid, which will try to keep rotating by its inertia, drags the photons so that $v_\gamma - v_b < 0$ if $v_{\gamma,\mathrm{ini}} > 0$. This argument is consistent with the result obtained from the tight coupling expansions, in other words, the magnetic fields generated by the first term in Eq. (16) are largely compensated by the second term. The resultant (comoving) magnetic fields spectrum has the characteristic cut-off at $k \gtrsim 1$ [Mpc^{-1}].

V. SUMMARY AND DISCUSSION

In this paper we examined observational constraints on the primordial vector mode discussed in [29]. This vector mode is a vector analogue of neutrino isocurvature velocity scalar mode [34] and has a non-decaying solution of
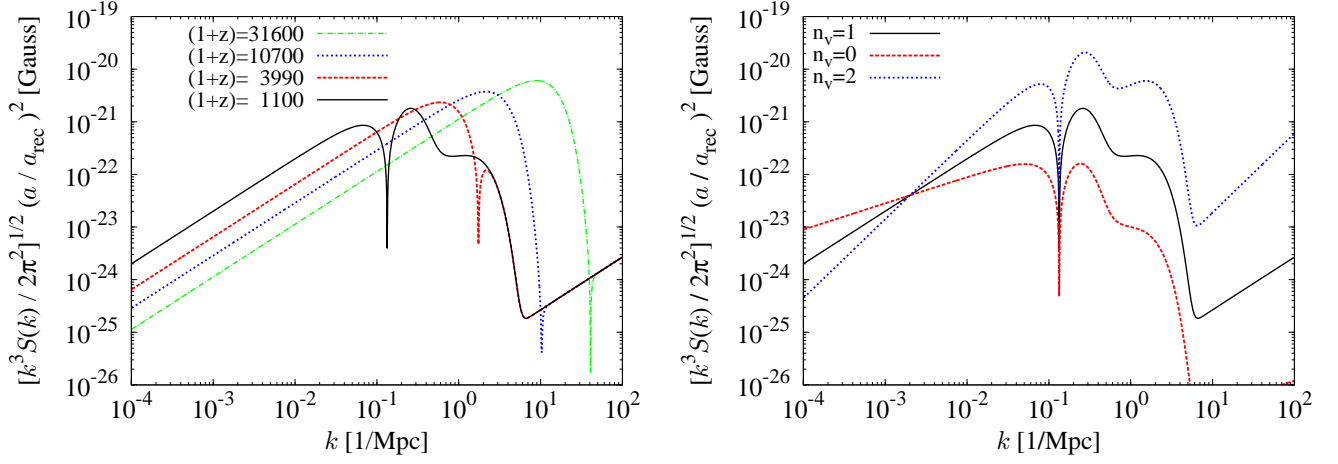
FIG. 4: Left: The spectra of magnetic fields generated from primordial vector modes at several times as indicated in the figure. The final spectrum at decoupling epoch is shown by the black solid line. Right: The dependence on n_v at $z = 1100$.
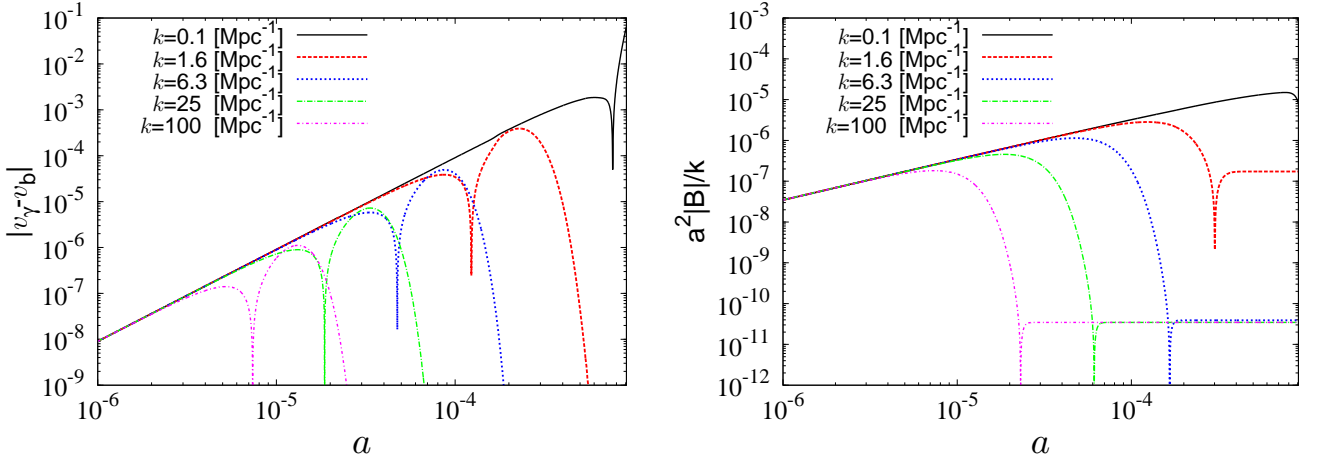

FIG. 5: Time evolutions of the source for the magnetic field (left) and the transfer of the magnetic field (right) for some wavenumbers as indicated. At first $v_\gamma - v_b = \alpha v_\gamma$ with $\alpha > 0$. This is because $v_\gamma \propto$ const. and $v_b \propto a^{-1}$ in the absence of interactions between photons and baryons, and therefore photons drag the baryons through Thomson interactions (the first term in Eq. (16)).

vector metric perturbation. The vector mode perturbations generate CMB angular anisotropies mainly through the Doppler effect, whose angular power spectrum is similar to that from the tensor mode without oscillatory features at small angular scales. Thus the amplitude of vector mode perturbations is constrained from CMB data. We used seven-year WMAP data to place a constraint on the vector-scalar ratio r_v. The constraint we obtained is $r_v \lesssim 0.01$ when the vector spectrum is nearly scale invariant. If the tensor mode is included the constraint is generalized to $r_v + (r/40) \lesssim 0.012$ where r is tensor-scalar ratio. The current constraint is placed mainly from the temperature anisotropy data. Future precise polarization data will tighten this bound significantly, down to $r_v \lesssim 10^{-3}$ for Planck [29].

As discussed by several authors, magnetic fields are generated before cosmological recombination through Compton scatterings if there existed cosmological vector mode perturbations. We numerically calculate the magnetic field spectrum generated from such primordial vector mode. We found that the spectrum is $B \approx 10^{-23}\text{G} \left(\frac{r_v}{0.01}\right)^{1/2} \left(\frac{k}{0.002}\right)^{(n_v+1)/2}$ at cosmological recombination where n_v is the spectral index of the primordial vector mode. The magnetic fields monotonically increases with wavenumber as $B \propto k^{(n_v+1)/2}$ up to the Silk damping scale. Below this scale we found that there is a non-trivial cancellation in the magnetic field generation, leading around five orders of magnitude decrease in the magnetic field amplitude. The cancellation occurs because the baryons drag the photons around the Silk damping epoch, before which, on the contrary, the photons dragged the baryons.

In fact, perhaps surprisingly, using the second order tight coupling approximation we can show that the magnetic

fields should eventually vanish at this order as follows. Deep in the radiation dominated era and at sub-horizon scales, the tight coupling equation of photon velocity is written as

$$v'_\gamma + \frac{k^2}{\dot\tau}\frac{4}{15}v_\gamma = 0 \ . \tag{35}$$

This equation can be solved to give the solution

$$v_\gamma = v_{\gamma,\text{ini}}\exp\left(-\frac{4k^2}{45\beta}\eta^3\right) \ , \tag{36}$$

where we have introduced a constant β to describe the differential optical depth as $\dot\tau \equiv \beta\eta^{-2}$ in the radiation dominated era. Inserting this solution into the tight coupling expression of the baryon-photon slip (Eq.(16)), and writing the time dependences of a, R and ρ_γ as $a = \alpha\eta$, $R = R_0\eta$ and $\rho_\gamma = \gamma\eta^{-4}$, respectively, the time integral to get the magnetic field amplitude can be expressed as

$$(a^2 B) \simeq \left(\frac{4\sigma_T k}{3e}\right)\int_{\eta_\text{ini}}^{\eta_\text{end}} a^2\rho_\gamma\delta v d\eta = \left(\frac{4\sigma_T k}{3e}\right)\int_{\eta_\text{ini}}^{\eta_\text{end}} \alpha^2\left(\frac{\gamma}{\beta}\right)R_0 v_{\gamma,\text{ini}}\left[1 - \frac{4}{15}k^2\beta\eta^3\exp\left(-\frac{4k^2}{45\beta}\eta^3\right)\right]d\eta \ . \tag{37}$$

The above integral of the form $\int_{\eta_\text{ini}}^{\eta_\text{end}}(1-K\eta^3)\exp(-K\eta^3/3)d\eta = \left[\eta\exp\left(-\frac{1}{3}K\eta^3\right)\right]_{\eta_\text{ini}}^{\eta_\text{end}}$ (with K constant) goes exactly to zero for $\eta_\text{ini} \to 0$ and $\eta_\text{end} \to \infty$.

The cancellation is perfect only within the second order tight coupling approximation in the completely radiation dominated era, and only when we integrate from $\eta = 0$ to $\eta = \infty$. Because we assume that the magnetic field generation starts at some finite time, $B(\eta_\text{ini}) = 0$ with $\eta_\text{ini} = \eta(z = 10^9)$, the surface term should remain as

$$a^2 B \simeq -\left(\frac{4\sigma_T k}{3e}\right)\alpha^2\gamma\left(\frac{R_0}{\beta}\right)v_{\gamma,\text{ini}}\eta_\text{ini} = -\left(\frac{4\sigma_T k}{3e}\right)a^2\rho_\gamma\frac{R}{\dot\tau}v_{\gamma,\text{ini}} \ . \tag{38}$$

We have found that the surface term above dominates the magnetic fields at small scales over the higher order terms in the tight coupling approximation, and indeed, our numerical solution is consistent with the above estimate at $k \gtrsim 10$ Mpc^{-1}. This suggests that the magnetic fields start to increase again with wavenumber as $B \propto k^{(n_v+1)/2}$ which is shown in Fig. 4. Consequently, magnetic fields will have a small-scale power up to $\sim 2 \times 10^{-3}$ pc in the comoving scale. This scale corresponds to the damping scale when the temperature of the universe was around MeV, after which epoch neutrinos can free-stream and the primordial vector mode solution considered here can apply.

The vector modes and magnetic fields considered in this paper are different from the recently investigated second order vector modes or magnetic fields [35–37]. In those studies the authors considered the second order vector modes and/or magnetic fields generated from the non-linear couplings of the first order scalar (density) modes. In the framework of the cosmological perturbation theory, the second order solution may be considered as a particular solution (in the limit of neglecting vector-scalar couplings), because the couplings of first order density modes can be considered as a source term for the otherwise homogeneous evolution equations of the vector mode. Therefore, the general solution may be expressed as a superposition of the solutions, namely, the second order solution and the solution considered in this paper. The second order solution suggests that magnetic fields generated in the second order vector modes have the amplitude as $B \approx 10^{-26}$ G around recombination at $k \approx 0.01$Mpc^{-1}. Comparing the amplitudes, the magnetic fields from the homogeneous solution considered in this paper will dominate the density perturbation induced magnetic fields if $r_v \gtrsim 10^{-8}$.

Another way to regularize the cosmological vector mode in the early universe will be a modification of the vector sector of gravity. An interesting example is Einstein-Aether theory which has been recently investigated with cosmological perturbations (see, e.g., [38, 39]). In this class of models the vector metric now becomes a dynamical variable, and the Aether field can induce another growing mode in the vector cosmological perturbations. It is expected that a sizable amount of vector type velocities in the fluids is induced [39]. The magnetic field generation from this vector mode will be an interesting subject, but beyond the scope of this paper.

In conclusion, in this paper it is found that the magnetic fields generated from the primordial vector mode at recombination are allowed at most $B \lesssim 10^{-21}$ G at $k \approx 0.1$ Mpc^{-1}. The upper bound comes from the upper bound on the primordial vector mode amplitude obtained from the seven-year WMAP data. This field amplitude is too small to be directly observed through Faraday effects on the distant radio sources and/or delays of high energy photons from gamma-ray bursts or blazars, however it may be large enough for the fields to be a seed for galactic magnetic fields observed today.

Acknowledgments

[1] L. M. Widrow, Reviews of Modern Physics **74**, 775 (2002).
[2] A.-C. Davis, M. Lilley, and O. Törnkvist, Phys. Rev. D **60**, 021301 (1999).
[3] M. L. Bernet, F. Miniati, S. J. Lilly, P. P. Kronberg, and M. Dessauges-Zavadsky, Nature **454**, 302 (2008), 0807.3347.
[4] L. Biermann and A. Schlüter, Physical Review **82**, 863 (1951).
[5] J. C. Kemp, Publ. Astron. Soc. Pac. **94**, 627 (1982).
[6] O. D. Miranda, M. Opher, and R. Opher, MNRAS **301**, 547 (1998).
[7] H. Hanayama et al., Astrophys. J. **633**, 941 (2005), astro-ph/0501538.
[8] G. Davies and L. M. Widrow, ApJ **540**, 755 (2000).
[9] R. M. Kulsrud, R. Cen, J. P. Ostriker, and D. Ryu, ApJ **480**, 481 (1997).
[10] N. Y. Gnedin, A. Ferrara, and E. G. Zweibel, ApJ **539**, 505 (2000).
[11] K. Subramanian, D. Narasimha, and S. M. Chitre, MNRAS **271**, L15+ (1994).
[12] B. Ratra, Astrophys. J. **391**, L1 (1992).
[13] K. Bamba and J. Yokoyama, Phys. Rev. **D69**, 043507 (2004), astro-ph/0310824.
[14] T. Prokopec and E. Puchwein, Phys. Rev. D **70**, 043004 (2004).
[15] M. S. Turner and L. M. Widrow, Phys. Rev. **D37**, 2743 (1988).
[16] V. Demozzi, V. Mukhanov, and H. Rubinstein, J. Cosmology Astropart. Phys. **8**, 25 (2009), 0907.1030.
[17] S. Kanno, J. Soda, and M. Watanabe, J. Cosmology Astropart. Phys. **12**, 9 (2009), 0908.3509.
[18] E. R. Harrison, MNRAS **147**, 279 (1970).
[19] S. Matarrese, S. Mollerach, A. Notari, and A. Riotto, Phys. Rev. D **71**, 043502 (2005).
[20] Z. Berezhiani and A. D. Dolgov, Astroparticle Physics **21**, 59 (2004).
[21] R. Gopal and S. K. Sethi, MNRAS **363**, 521 (2005).
[22] K. Takahashi, K. Ichiki, H. Ohno, and H. Hanayama, Physical Review Letters **95**, 121301 (2005), arXiv:astro-ph/0502283.
[23] K. Ichiki, K. Takahashi, H. Ohno, H. Hanayama, and N. Sugiyama, Science **311**, 827 (2006), arXiv:astro-ph/0603631.
[24] E. Fenu, C. Pitrou, and R. Maartens, MNRAS **414**, 2354 (2011), 1012.2958.
[25] K. Ichiki, K. Takahashi, N. Sugiyama, H. Hanayama, and H. Ohno, ArXiv Astrophysics e-prints (2007), arXiv:astro-ph/0701329.
[26] S. Maeda, S. Kitagawa, T. Kobayashi, and T. Shiromizu, Classical and Quantum Gravity **26**, 135014 (2009), 0805.0169.
[27] E. R. Siegel and J. N. Fry, ApJ **651**, 627 (2006), arXiv:astro-ph/0604526.
[28] A. Rebhan, ApJ **392**, 385 (1992).
[29] A. Lewis, Phys. Rev. D **70**, 043518 (2004), arXiv:astro-ph/0403583.
[30] N. Jarosik, C. L. Bennett, J. Dunkley, B. Gold, M. R. Greason, M. Halpern, R. S. Hill, G. Hinshaw, A. Kogut, E. Komatsu, et al., ApJS **192**, 14 (2011), 1001.4744.
[31] D. Larson, J. Dunkley, G. Hinshaw, E. Komatsu, M. R. Nolta, C. L. Bennett, B. Gold, M. Halpern, R. S. Hill, N. Jarosik, et al., ApJS **192**, 16 (2011), 1001.4635.
[32] A. Lewis, A. Challinor, and A. Lasenby, Astrophys. J. **538**, 473 (2000), astro-ph/9911177.
[33] W. Hu and N. Sugiyama, ApJ **444**, 489 (1995), arXiv:astro-ph/9407093.
[34] M. Bucher, K. Moodley, and N. Turok, Phys. Rev. D **62**, 083508 (2000), arXiv:astro-ph/9904231.
[35] T. Lu, K. Ananda, and C. Clarkson, Phys. Rev. D **77**, 043523 (2008), 0709.1619.
[36] T. Lu, K. Ananda, C. Clarkson, and R. Maartens, J. Cosmology Astropart. Phys. **2**, 23 (2009).
[37] A. J. Christopherson, K. A. Malik, and D. R. Matravers, ArXiv e-prints (2010), 1008.4866.
[38] C. Armendariz-Picon, N. Fariña Sierra, and J. Garriga, J. Cosmology Astropart. Phys. **7**, 10 (2010), 1003.1283.
[39] M. Nakashima and T. Kobayashi, Phys. Rev. D **84**, 084051 (2011), 1103.2197.